



# IMPACT DAMAGE EVALUATION OF GLASS-FIBER REINFORCED POLYMER (GFRP) USING THE DROP TEST RIG – AN EXPERIMENTAL BASED APPROACH

S. N. A. Safri, M. T. H. Sultan and F. Cardona

Aerospace Manufacturing Research Centre, Faculty of Engineering, Universiti Putra Malaysia, Selangor Darul Ehsan, Malaysia

E-Mail: [snasafri@gmail.com](mailto:snasafri@gmail.com)

## ABSTRACT

The experimental results of low-energy drop-weight impact tests on woven-roving Glass Fiber Reinforced Polymer (GFRP) type C-glass/Epoxy 600 g/m<sup>2</sup> and Type E-glass/Epoxy 800 g/m<sup>2</sup> are presented. The effects of specimen thickness based on the number of plies and impact energy are investigated. Impact damage and response was observed for eight levels of impact energies, 6, 12, 18, 24, 30, 36, 42 and 48 J. From the experimental studies, it can be concluded that for each type of GFRP, the impact energy showed excellent correlation with the impact response. The difference in the number of plies fabricated and the mechanical properties for both types of GFRP do affect the impact response and impact damage of the specimens tested. It can be concluded that GFRP type E-800 is higher in strength compared to GFRP type C-600.

**Keywords:** glass fiber reinforced polymer, low velocity impact, drop weight test, fiberglass, impact damage.

## INTRODUCTION

Composites are well known for their excellent weight/strength and weight/stiffness properties and they are the materials of choice for light-weight structures. Fiber Reinforced Plastics (FRP) composites are widely used in aircraft components such as spoilers, wings and in subsystems such as turboprops and turbofans. Composites have now replaced light alloys in aircraft components since they are lighter and have a lower maintenance control surface (cleaning and polishing). Laminated fiber-reinforced composite materials are also known for their good environmental resistance and fatigue resistance. Glass Fiber Reinforced Polymer (GFRP), Carbon Fiber Reinforced Polymer (CFRP), Kevlar and hybrid composites are commonly used for aircraft structures and components. However, these materials are at risk of experiencing damage.

There are different types of damage possible in an aircraft such as fatigue, corrosion, accidental (impact) damage, and associated repairs; it is reported that at least 13% of 688 repairs to 71 Boeing 747 fuselages were related to impact damage [1]. Impact damage is an important type of failure in aircraft structures. Vlot [2] reported that impact damage is usually located around the doors, on the nose of the aircraft, in the cargo compartments and at the tail (due to tail scrape over the runway). Impact damage on aircraft is caused by sources such as: runway debris (in the order of 60 m/s), hail (on the ground 25 cm and 60 m/s and in flight in the order of hundreds of meters per second), maintenance damage or dropped tools (less than 10 m/s), collisions between service cars or cargo and the structure (the velocity is low), bird strikes (high velocities), ice from propellers striking the fuselage, engine debris, and ballistic impact (for military aircraft) [2]. Impact damage occurs due to impact loading on the structure.

## Fibreglass

In general, fibreglass is a low cost material and has good electrical insulation. However, it has a short fatigue life due to the low stiffness of glass reinforcement. In a humid environment, the strength of fibreglass is reduced under sustained loading, as the moisture absorbed onto the surface of the flaw reduces the surface energy. Glass fiber is commonly chosen in impact sensitive applications even though it has a lower elastic modulus and lower resistance to fatigue. It has the higher impact damage tolerance of laminates and a lower raw material cost compared to carbon fibers [3-5]. GFRP laminate has great impact resistance since it has higher energy absorption due to its higher strain to failure ratio compared to a carbon fiber reinforced material [6, 7]. Table-1 shows the mechanical properties of C-glass and E-glass [8]. The density, tensile strength and modulus of elasticity of E-glass is higher than that of C-glass.

**Table-1.** Mechanical properties of C-glass and E-glass [8].

Property	C-glass	E-glass
Density (g/cm <sup>3</sup> )	2.52	2.58
Tensile strength at 23°C (MPa)	3310	3445
Young's modulus at 23°C (GPa)	68.9	72.3
Elongation percentage	4.8	4.8

Type E- glass fiber with a mass of 800 g/m<sup>2</sup> is thicker compared to Type C-glass fiber with a mass of 600 g/m<sup>2</sup>. The hardness of Type E fiber with a mass of 800 g/m<sup>2</sup> is high compared to Type C fiber with a mass of 600 g/m<sup>2</sup> since its fiber composition is greater. There are only a few research studies that have been done on Type C-glass/Epoxy 600g/m<sup>2</sup> and Type E-glass/Epoxy 800 g/m<sup>2</sup>. This paper investigates the low-velocity impact behaviour of GFRP Type E-glass/epoxy and Type C-glass/epoxy



reinforced composites, so that GFRP usage can be widened in aircraft structures. There have been similar work done before using drop test rig to evaluate impact damage. However, none of the work is comparing between this two material GFRP type C-glass/Epoxy 600 g/m<sup>2</sup> and Type E-glass/Epoxy 800 g/m<sup>2</sup>.

### Low velocity impact

There are a few categories of impact loading, and specifically these are: low velocity (large mass), intermediate velocity, high/ballistic velocity (small mass), and hyper velocity impact. Low velocity impacts occur at a velocity below 10 m/s, intermediate impacts occur at 10 m/s and 50 m/s, high velocity (ballistic) impacts have a range of velocity from 50 m/s to 1000 m/s, and hyper velocity impacts have the range of 2000 m/s to 5000 m/s [9]. Sjoblom *et al.* [10] and Shivakumar *et al.* [11] defined low velocity impacts as events which can occur in the range 1–10 m/s depending on the target stiffness, material properties and the impactor mass and stiffness. A low velocity impact event can occur in-service or during maintenance activities and can be considered one of the most dangerous loads on composite laminates. It is an unsafe type of load since it affects the performance of composites.

For low velocity impact events, the use of pendulums like the ones present in the Charpy test, the Izod test and drop towers or drop weights have become standard. A drop weight impact testing unit enables the simulation of a wide variety of real-world impact conditions and collects detailed performance data [12]. One of the advantages of this test with respect to the Charpy and Izod tests is that a wider range of test geometries can be examined, thereby enabling more complex components to be tested [13]. In this paper, although testing is generally undertaken using a hemispherical impactor, it is possible to use other impactor shapes such as blunt cylinders or sharp points.

### Non-destructive testing

According to a composite aircraft design handbook [14], damage criteria are classified into five categories depending on the severity of the damage. The first category is barely visible impact damage (BVID), and the second category is visible impact damage (VID). Visible impact damage (VID) is a clear damage on the specimen that can be easily seen using the naked eye. Barely visible impact damage (BVID) is damage that can seldom be seen using the naked eye. Both types of damage can be evaluated using post impact testing. There are various methods available for detecting impact damage such as X-ray [15], C-scan [16, 17], Scanning Electron Microscope (SEM) [18, 19], dye penetrant and optical microscope. It is essential to determine the existence and location of the damage. Typically, by carrying out visual observation directly on the impacted surface, the presence of matrix cracks and the size and shape of delamination can be predicted. In this research, the damage experienced by the impacted specimen are BVID and VID.

## EXPERIMENTAL PROCEDURE

### Preparations of specimen

The composite materials chosen are woven roving Glass Fibre Reinforced Polymer (GFRP) type C-glass/Epoxy 600 g/m<sup>2</sup> and type E-glass/Epoxy 800 g/m<sup>2</sup>. These woven roving materials were laminated with resin to increase their impact strength. The materials were fabricated using a hand lay-up technique with the aid of rollers. The process of preparing the compound is based on a 2:1 ratio: that is, 2 portions of epoxy to 1 portion of hardener. The epoxy resin and hardener used are from types Zeepoxy HL002TA and Zeepoxy HL002TB. For each thickness, five panels of 350mm×350mm were laminated. After the hand lay-up process, the top layer of laminate was covered with glass and four 150N weights were placed on the top of the glass. The curing process was carried out at room temperature for 48 hours. 120 specimen plates as per the Boeing Specification Support Standard BSS 7260 (100mm×150mm) for both types were cut using a CNC Router Machine. The thickness for each material is shown in Table-2.

**Table-2.** Laminate thickness for type C-glass/Epoxy 600 g/m<sup>2</sup> and type E-glass/Epoxy 800 g/m<sup>2</sup>.

Type of Fibreglass	Number of plies	Average Thickness, (mm)
C-glass/Epoxy 600 g/m <sup>2</sup>	10	6.0 ± 0.10
	12	7.0 ± 0.12
	14	8.0 ± 0.09
E-glass/Epoxy 800 g/m <sup>2</sup>	10	7.0 ± 0.11
	12	8.0 ± 0.10
	14	9.0 ± 0.12

Table-2 compares the average thicknesses of the laminates. The thickness are measured after the curing process. The standard deviation are the same since the thickness of the fabricated specimen is almost the same. This is because the same procedure has been used to fabricate the specimen. It shows that GFRP type E-glass/Epoxy 800 g/m<sup>2</sup> produced much thicker laminates compared to type C-glass/Epoxy 600 g/m<sup>2</sup> for the same number of plies. Tests were performed on different sample thicknesses to achieve different impact responses.

### Impact test configurations

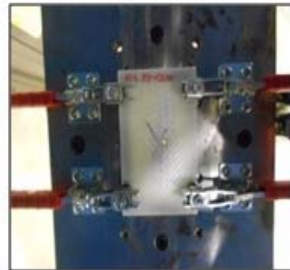
The Drop Weight Impact test was performed using an instrumented falling-weight-impact test machine, IMATEK IM10T, at International Islam University Malaysia (IIUM). This was integrated with software, IMATEK Impact Analysis, to acquire impact results data. The tests were achieved by dropping a striker attached to a variable weight onto the sample and at an arranged impact velocity. The software performs its calculations from the basic force-time information, velocity, displacement and energy absorbed by the specimen. There are three main parts to the drop-weight apparatus, a tower where the



weight falls onto the sample held below, a control unit, and the computer software system as shown in Figure-1.



Tower



The sample and the clamp

**Figure-1.** Parts of the drop weight apparatus. The specimen was tightly clamped at four corners during the impact test. All tests were conducted at room temperature.

The tower consists of a sample area, where there are four clamps holding the sample, and a column from which an impactor head attached to a weight falls onto the sample. The striker was 0.787 kg in weight, and had a hemispherical geometry in shape, with a tip radius of 5 mm. The total drop mass is 8.891 kg. Two types of GFRP, type C-glass/Epoxy 600 g/m<sup>2</sup> and type E-glass/Epoxy 800 g/m<sup>2</sup> with three thicknesses of laminate, 10, 12 and 14 plies, were considered. The variable used to define the magnitude of the impact event is the impact energy. The low velocity impact response of the samples was investigated at different impact energies in order to evaluate the capability of the laminates to dissipate the impact energy.

For the 12-ply and 14-ply specimens, for both types of GFRP, a total of 96 plates were used in the impact tests at 8 different energy levels. The impact energies are chosen because before the actual test, there is a test had been done earlier to know the maximum impact energy that can be sustained by the specimen. At impact energy more than 48J, for specimen with 10 number of plies, penetration will occur. Therefore, the impact energy chosen for this research are from 6J to 48J. These impact energies give a velocity ranging from 1.6m/s to 3.3 m/s and these velocity ranges are in the range of low velocity impact as has been explained in the literature. The impact energies for the 12-ply and 14-ply specimens were 6, 12, 18, 24, 30, 36, 42, and 48 J. However, for 10-ply specimens, for both types of GFRP, a total of 24 plates were used to perform the impact test at four energy levels, 12 J, 24 J, 36 J, and 48 J due to material and cost limitations. For each type of energy, three samples were subjected to impact respectively to obtain data repeatability. The reason for performing the repeatability test was to check the accuracy of the measurements.

In order to obtain different energy levels, the height from which the impactor should be released was calculated theoretically. The same drop mass was used for

all the tests, 8.891 kg, and the impact energy of the drop was obtained using Equation(1) [20]:

$$E_I = m \cdot g \cdot h. \quad (1)$$

It was found that the height should be 0.069 m for an impact energy of 6 J. For 12, 18, 24, 30, 36, 42 and 48 J, the corresponding height for the impactor to be released was 0.138, 0.206, 0.275, 0.344, 0.413, 0.482, and 0.551 m. Equation(1) shows that the drop height increased with increasing impact energy. The impactor mass together with the height of the drop determines the energy of the impacts. The specimens were impacted at the midpoint using a hemispherical shaped impactor.

The characterization of the impact tests was based on the conservation of energy principle where the potential energy (PE) before the impact event is assumed to be equal to the kinetic energy (KE) after the impact event [21, 22]. The initial velocity of the impactor,  $v$ , can be calculated using Equation(2) where  $g$  is gravitational acceleration, 9.81 [ms]<sup>-2</sup>, and  $h$  is the impactor height.

$$v = \sqrt{2gh} \quad (2)$$

It was found that for an impact energy of 6, 12, 18, 24, 30, 36, 42 and 48 J, the initial velocity of the impactor is 1.1, 1.6, 2.0, 2.3, 2.6, 2.8, 3.0, and 3.3 [ms]<sup>-1</sup>. The velocities calculated are the same as the velocities setup using the drop test machine. These velocities are still in the range of low velocity impact events as has been explained earlier in the literature.

#### Non-Destructive Evaluation

The low velocity impact damage on the specimen was examined using the dye penetrant technique and an optical microscope. The basic theory of liquid penetrant testing is capillary action, which allows the penetrant to enter in the gap of damage, remain there when the liquid is removed from the material surface, and then re-emerge on the surface on application of a developer, which has a capillary action similar to blotting paper [23]. It is a very effective test method since inspection can be carried out without any additional visual aid. Dye penetrant will go into the smallest crack experienced by the specimen due to the impact event (even into micro-cracks, it just take longer time for the dye penetration to occur). After the dye penetrant test, the damage on the specimen becomes clearer. Therefore, it is much easier to calculate the damage area. After the dye penetrant test, the damage area has been drawn on the specimen before the drawing was copied to graph paper. Then, the damage drawing was then calculated.

The dye penetrant used was Spotcheck SKL-SP2 dye penetrant. It has a solvent removable (or post emulsifiable) red colour contrast penetrant with outstanding penetrating characteristics. Spotcheck SKL-SP2 is compliant with ASME B & PV Code Sec V and the ASTM E1417 standard. All impacted specimens were

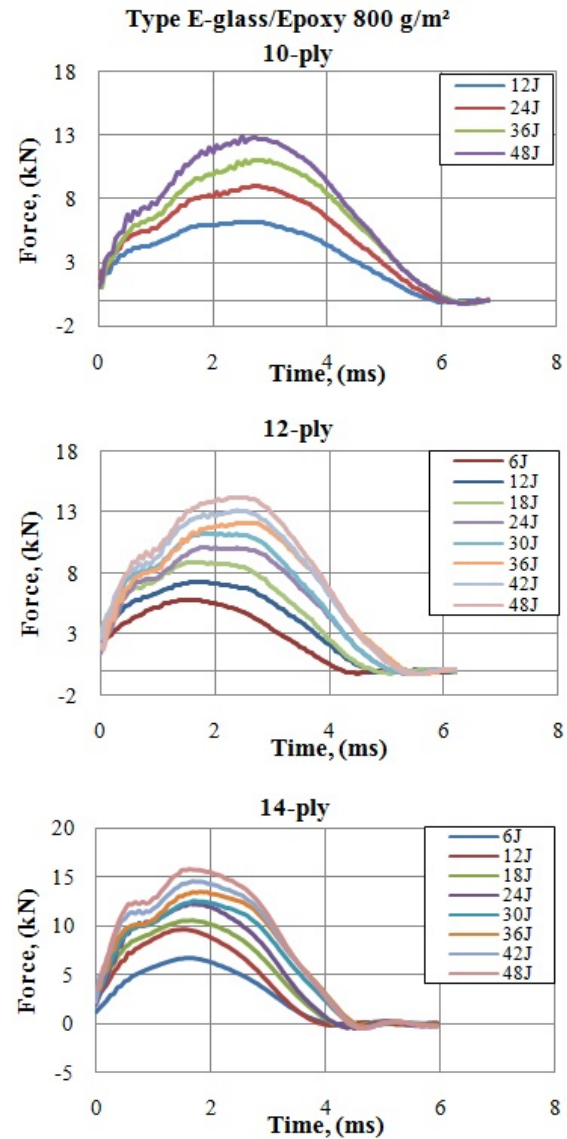
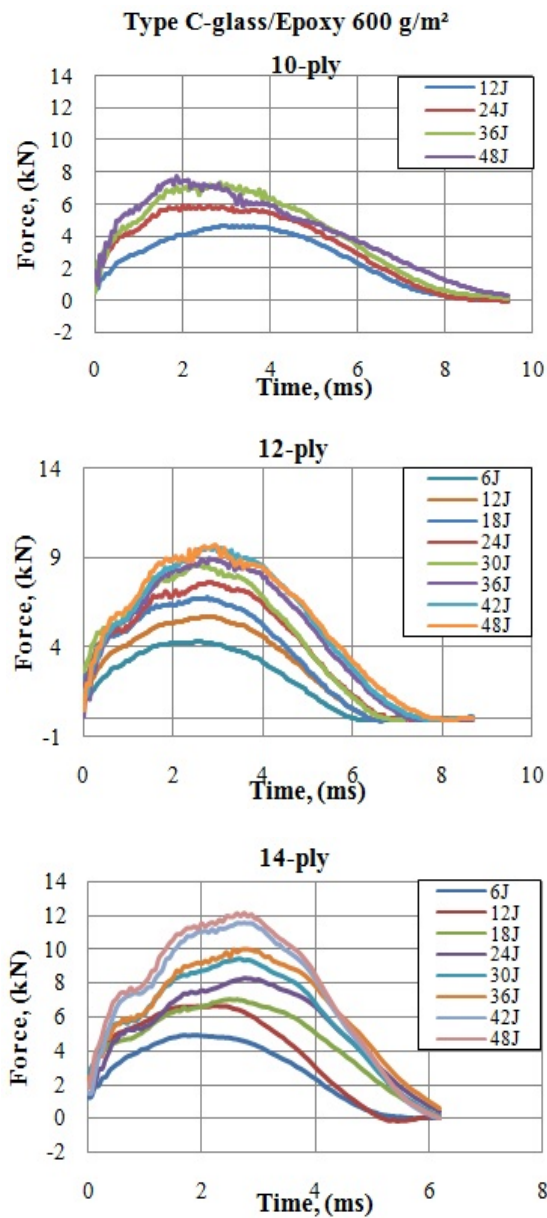




cleaned using a thinner. Dye penetrant was applied onto the specimen. After the specimen was left for penetration for about 20 minutes, all excessive dye penetrant was cleaned using a thinner. Optical microscopy was also used to investigate the impact damage in the laminates. Delamination, matrix cracking, matrix breakage, fiber cracking, and fiber breakage were observed from the microstructure of the damaged specimens.

## RESULTS

### Impact force analysis



**Figure-2.** Force-time history plots for 10, 12 and 14-ply type C-glass/Epoxy 600 g/m<sup>2</sup> (left) and type E-glass/Epoxy 800 g/m<sup>2</sup> (right).

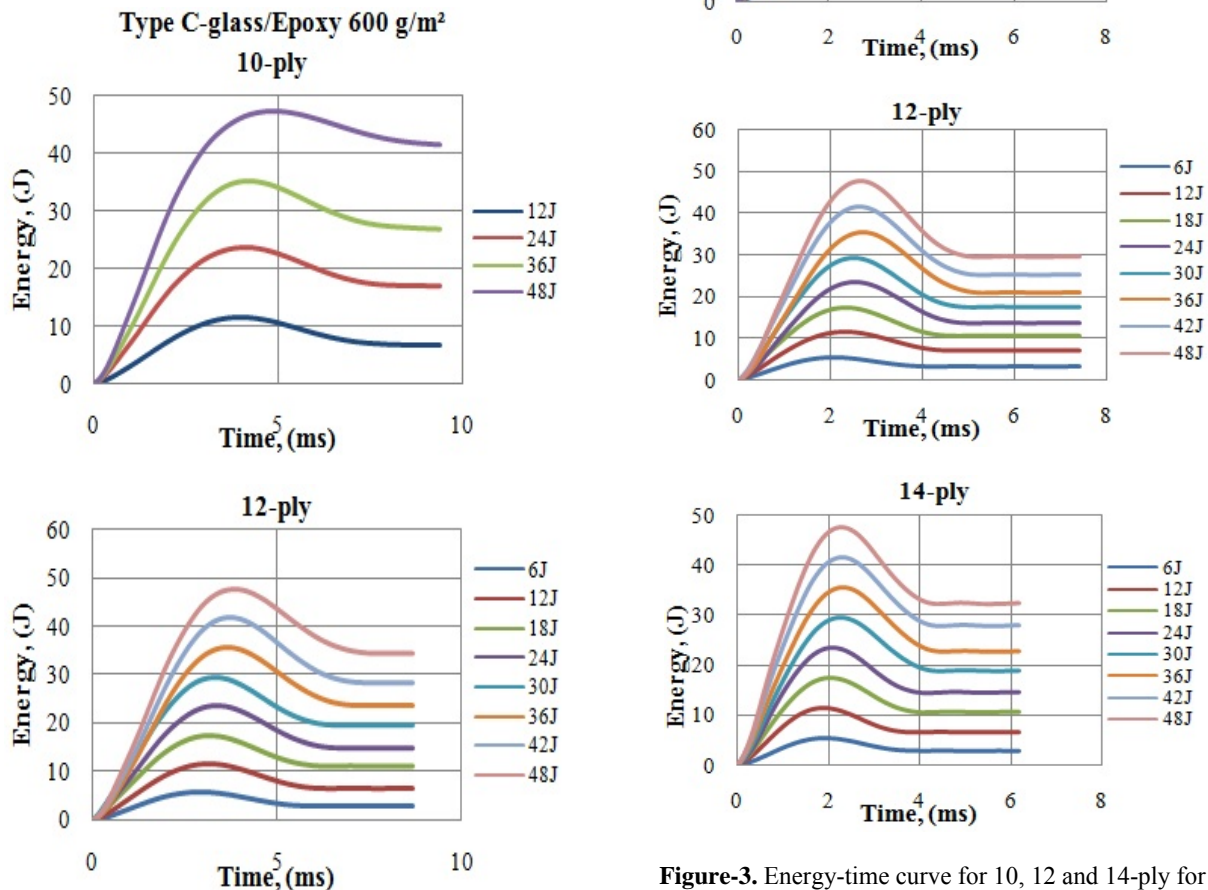
The force time history plots at 6, 12, 18, 24, 30, 36, 42, and 48 J of impact energy for the average of each set of samples at each energy are shown in Figure-2. These diagrams represent a typical behaviour and are in agreement as reported in the literature [24]. The force-time history can yield significant information pertaining to damage initiation and growth [25, 26]. As the tested energy increases, the peak forces increase with energy as expected. It is possible to observe that the force increases up to a maximum value followed by a drop corresponding to the impactor rebound. Both types of GFRP show that as the number of plies increases, the peak force also increases. The curve shows that GFRP type C-glass/Epoxy 600 g/m<sup>2</sup> has a lower value of peak force for all numbers of plies compared to type E-glass/Epoxy 800 g/m<sup>2</sup>. All the



curves are not smooth, and a major load drop occurs and is followed by multiple cycles of loading and partial unloading before the final unloading. The peak load increases greatly and the contact time increases slightly with the impact energy, while the load at which the major load drop occurs (if there is any) is almost the same for all impact energy levels.

The force plot is not smooth because it indicates damage experienced by the specimen. GFRP type C-glass/Epoxy 600 g/m<sup>2</sup> curves are not smooth, and a major load drop occurs and is followed by multiple cycles of loading and partial unloading before the final unloading. The oscillation indicates the existence of damage progression. A smooth curve signifies a more severe damage [27]. There are more oscillations (irregular behaviour) in the curve of GFRP type C-glass/Epoxy 600 g/m<sup>2</sup> compared to GFRP type E-glass/Epoxy 800 g/m<sup>2</sup> because the damage from the incident impact is more severe for GFRP type C-glass/Epoxy 600 g/m<sup>2</sup>. The peak load increased greatly and the contact time increased slightly with the impact energy, while the load at which the major load drop occurred (if there is any) is almost the same for all impact energy levels.

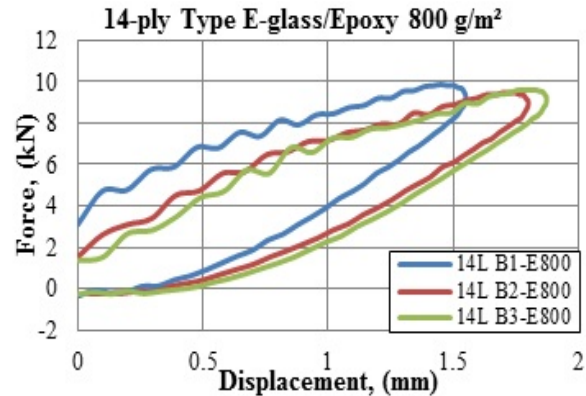
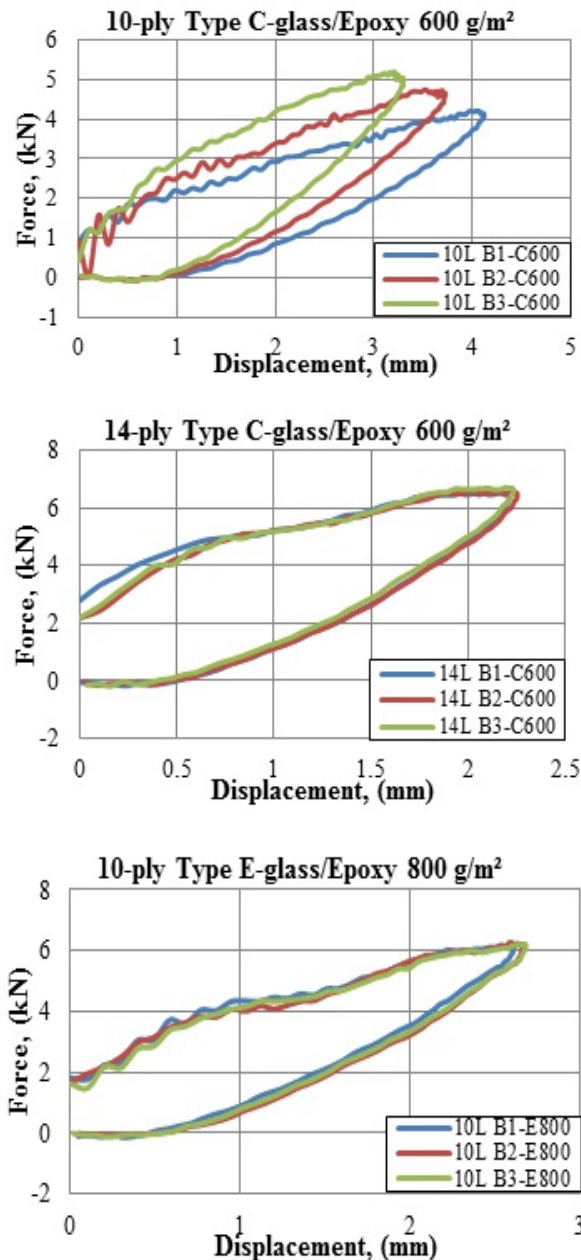
#### Energy absorbed analysis



**Figure-3.** Energy-time curve for 10, 12 and 14-ply for type C-glass/Epoxy 600 g/m<sup>2</sup> and type E-glass/Epoxy 800 g/m<sup>2</sup>.

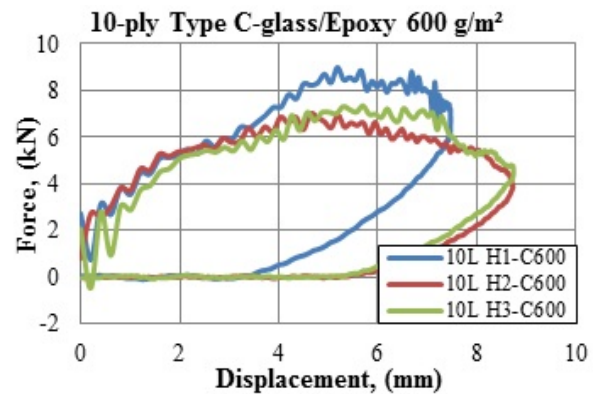


Figure-3 shows that for both types of GFRP, the energy level increases slowly up to it speak. Both types of GFRP possess the same trend of energy curve. The absorbed energy of the material can be analyzed from the energy-time curve [9]. The absorbed energy is the energy level at which the curve becomes constant with time. The absorbed energy increases with an increase in the impact energy. The energy-time curves show specimens energy dissipation. Roughly 50% of the energy was returned. This means that the composite works in elastic region and experience phenomena such as delamination or matrix cracking.

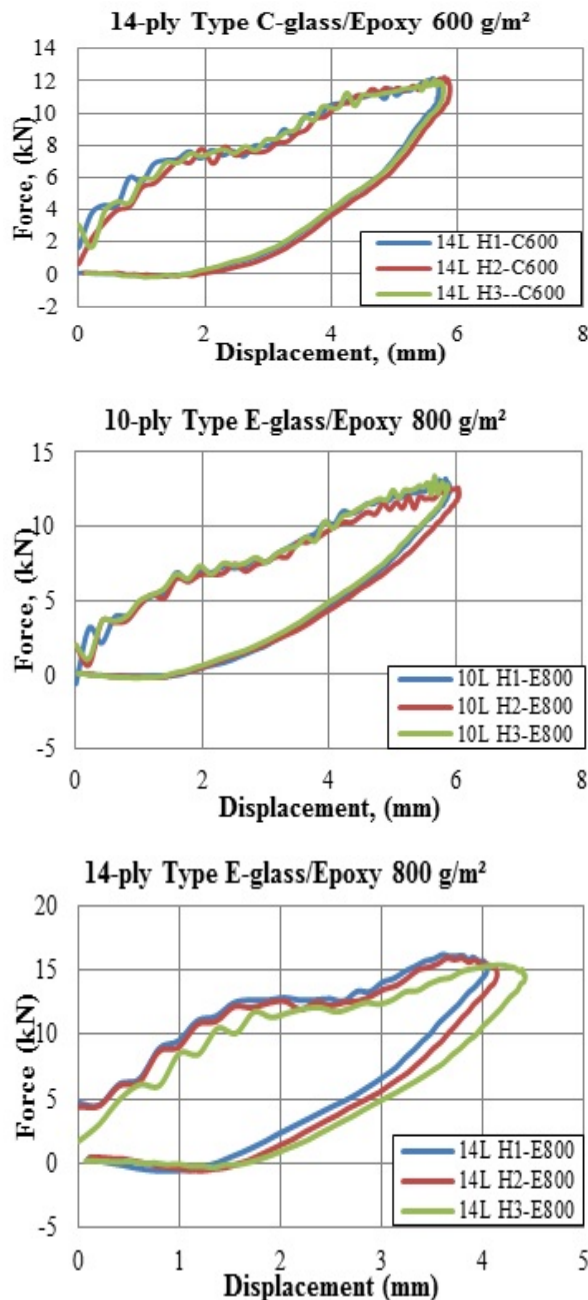


**Figure-4.** Force-displacement curve at impact energy 12J for type C-glass/Epoxy 600 g/m<sup>2</sup> and type E-glass/Epoxy 800 g/m<sup>2</sup>.

The type of GFRP and the number of plies effect on the impact response of woven fabric composite plates is examined experimentally. Force-displacement curves contain important information about the damage progression in an impact event. The displacement term here indicates the movement of the impactor and the deflection of the impacted surface of the sample during contact between the specimens and the impactor. There are two types of curves, the closed curve and the open curve [28]. A closed curve consists of an ascending section of loading and a descending section combining loading and unloading, in general. If the descending section is completely a softening curve, open curve, the force-displacement curve may represent either penetration or perforation cases. Figure-4 shows the force displacement curve at impact energy 12 J and Figure-5 shows the force displacement curve at impact energy 48 J.





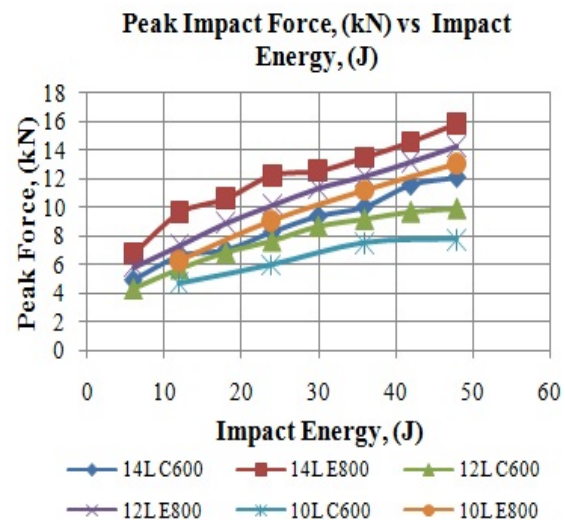


**Figure-5.** Force-displacement curve at impact energy 48 J for type C-glass/Epoxy 600 g/m<sup>2</sup> and type E-glass/Epoxy 800 g/m<sup>2</sup>.

From Figure-4 and Figure-5, it is seen that the force-displacement curve has ascending and descending sections. The slope of the ascending section of the curves is named the impact bending stiffness. The highest value reached in the force-displacement curves is called the peak force [29]. Returning toward the origin of the diagram following the descending section indicates the rebounding of the impactor from the specimen surface after impact.

Only the force-displacement curve for 10-ply and 14-ply for both materials is shown because the graph pattern was the same for the 12-ply specimens. Impact energies of 12 J and 48 J were chosen in this graph in order to compare between the impact energies tested for both types of GFRP. The maximum deflection can be found from the graph at the point when the force curve returns to zero [30]. The maximum deflection of the impacted specimen can be seen as in Figure-10. The absorbed energy of the specimen can be determined by calculating the area enveloped by the force-displacement curve.

#### Variation of maximum impact force and impact energy



**Figure-6.** Peak impact force-impact energy curve for type C-glass/Epoxy 600 g/m<sup>2</sup> and type E-glass/Epoxy 800 g/m<sup>2</sup>.

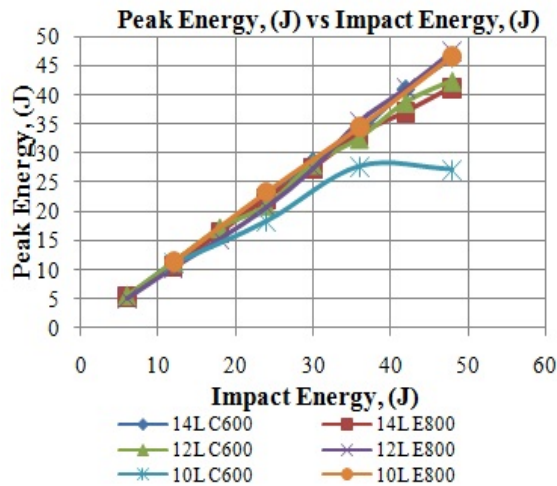
Figure-6 shows that the average peak impact force is found to follow the same increasing trend with respect to impact energy, regardless of the type of material and the number of plies. The impact force is dependent on the input energy and target stiffness. The impact force is dependent on the input energy and target stiffness. This is because, as the impact energy increased, the impact force also increases and these can be seen from the data collected from the test. As the target stiffness increases, the impact force also increases. This is because more forces is required to initiate damage on the specimens. Stiffness is a characteristic of the panel system including materials, thickness, and boundary conditions.

The impact forces generated for impacts onto the 14-ply type E-glass/Epoxy 800 g/m<sup>2</sup> are significantly larger than for all other tested specimens due to its high stiffness. This shows that GFRP type E-glass/Epoxy 800 g/m<sup>2</sup> is stiffer than GFRP type C-glass/Epoxy 600 g/m<sup>2</sup>. It can be stated that the greater the peak impact forces, the stiffer the projectile-to-target interactions. This resulted in shorter contact duration, and more rapid load increases up to the maximum values [31]. All eight different impact



energy levels were tested and the results reveal that the measured peak impact force shows an excellent correlation with impact energy. It is also seen from Figure-6 that GFRP type E-glass/Epoxy 800 g/m<sup>2</sup> experiences a higher peak impact force compared to GFRP type C-glass/Epoxy 600 g/m<sup>2</sup> for all thicknesses.

#### Variation of peak energy and impact energy



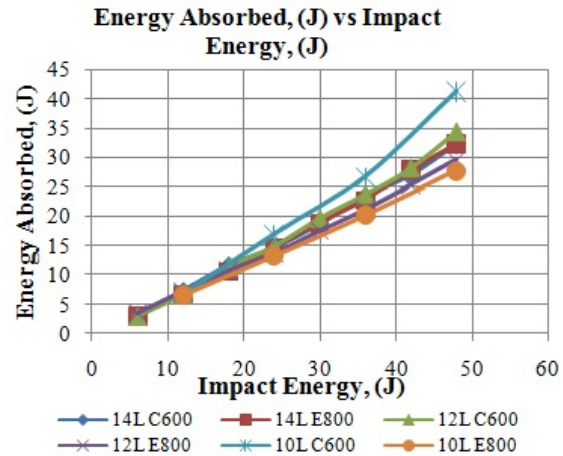
**Figure-7.** Peak energy-impact energy curve for type C-glass/Epoxy 600 g/m<sup>2</sup> and type E-glass/Epoxy 800 g/m<sup>2</sup>.

Peak energy consists of the energy absorbed via the elastic deformation of the specimen and the energy dissipated via damage initiation and propagation. For non-penetration impact events, the peak energy is invariably higher than the energy at failure due to elastic recovery when the striker bounces upwards [32]. Figure-7 shows the peak energy-impact energy curve for both types of GFRP. It can be seen that as the impact energy increases, the peak energy increases too. However, for 10-ply type C-glass/Epoxy 600 g/m<sup>2</sup>, the value of the peak energy is decreasing at 48 J. This is because, at 48 J, penetration almost occurs at the tested specimen.

#### Variation of energy absorbed and impact energy

Impact energy and absorbed energy are two important parameters to assess the impact response and resistance of composite structures. The absorbed energies are a fraction of the impact energy which is absorbed by the structure and is not transformed on the elastic energy [33]. Thus, each failure mechanism - matrix crack, intra-layer failures, delamination, fibre breakage - absorbs a fraction of the impact energy. Therefore, the amount and the type of the failure mechanisms activated will affect the total absorbed energy values. However, the amount and the type of the failure mechanisms activated depend on the mechanical properties of the fibre, the core and the matrix used for the manufacturing of the sandwich structure, the shape of the impactor head, the orientation of the fibre

layers, the geometry of the specimen, and the impact energy level.

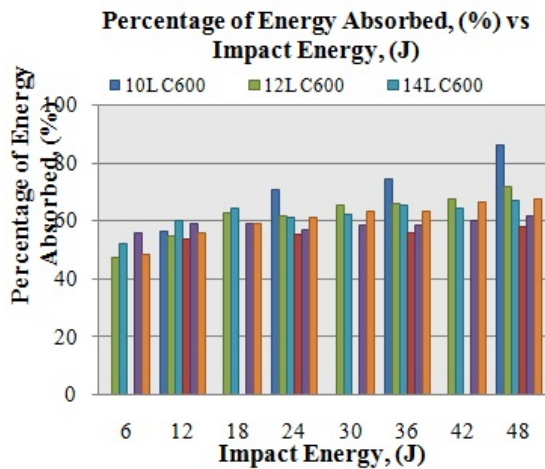


**Figure-8.** Energy absorbed-impact energy curve for type C-glass/Epoxy 600 g/m<sup>2</sup> and type E-glass/Epoxy 800 g/m<sup>2</sup>.

In the present study, the mechanical properties of the fibre used for the manufacturing of the laminates and the impact energy level, were seen as the major causes of the variation in total energy absorption. Figure-8 shows that 10-ply type C-glass/Epoxy 600 g/m<sup>2</sup> specimens have better energy absorption capabilities than 10-ply type E-glass/Epoxy 800 g/m<sup>2</sup>. The absorbed energy was obtained by calculating the area under the graph of force-displacement from Figure-4 and Figure-5. It is notable to state that as the impact energy increases, the energy absorbed by the specimens is also increasing. It is shown that as the impact energy increases, the energy absorbed increases because the Young's moduli of the GFRP laminates increases. This is because GFRP type E-glass/Epoxy 800 g/m<sup>2</sup> is already known to have higher Young's modulus than GFRP C-glass/Epoxy 600 g/m<sup>2</sup>. Young's modulus is a measure of the stiffness of an elastic material. Higher elastic modulus means the material is stiffer.

A qualitatively similar correlation between impact energy and energy absorbed was found by Sutherland et al [34]. Sikarwar et al [35] states that as the laminate thickness increases, the resistance offered by the laminates in delaminations increases and absorbs more energy in delaminations mode.

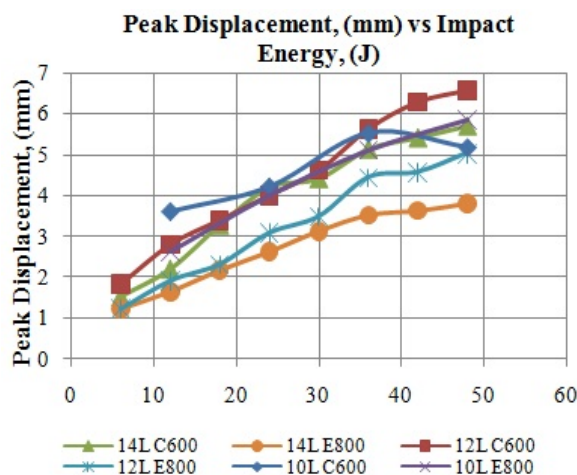




**Figure-9.** Percentage of energy absorbed-impact energy curve for type C-glass/Epoxy 600 g/m<sup>2</sup> and type E-glass/Epoxy 800 g/m<sup>2</sup>.

The total energy is composed of the energy absorbed by the laminate and the elastic energy loss [9]. If a percentage of the energy absorbed is high, the energy converted to elastic energy is low. This means more failure mechanisms. Figure-9 shows that at 6 J, 12-ply type E-glass/Epoxy 800 g/m<sup>2</sup> has the highest percentage of absorbed energy, which is 56%, and 14-ply Type E-glass/Epoxy 800 g/m<sup>2</sup> has the lowest percentage of absorbed energy, which is 48%. The lower energy absorption means that there is not much energy lost due to failure. At 48 J of impact energy, 10-ply type C-glass/Epoxy 600 g/m<sup>2</sup> has the highest percentage of energy absorbed, which is 86%, while 10-ply type E-glass/Epoxy 800 g/m<sup>2</sup> has the lowest percentage of energy absorbed, which is 57%.

#### Variation of peak displacement and impact energy



**Figure-10:** Peak displacement-impact energy for type C-glass/Epoxy 600 g/m<sup>2</sup> and type E-glass/Epoxy 800 g/m<sup>2</sup>.

Figure-10 shows that the peak displacement increases with increasing impact energy values for the tests for both types of GFRP. The displacement value is obtained from the data acquisition system attached together with the drop weight tester. The general shape of the impact energy versus deflection curves is similar for all tests. GFRP type E-800 has higher strength compared to GFRP type C-600 as shown in Table-1. Therefore, it can sustain higher impact energy compared to GFRP type C-600. Peak displacement indicates the maximum deflection of the specimen. It implies that there is a higher amount of damaged fibres due to increased impact energies. Therefore, it can be concluded that GFRP type C-600 had experienced more damage compared to GFRP type E-800.

#### NON-DESTRUCTIVE TESTING

##### Dye penetrant damage detection

Dye penetrants were used for detecting visible impact damage (VID). Dye-penetrant helps to raise the visibility of damage. The low velocity impact damage was examined by means of visual observation using dye penetrant. In all specimens, delamination was clearly visible to the naked eye. For a low-velocity impact, damage starts with the creation of a matrix crack [36].

**Table-3.** Damage area at impact energy 12 J for C-glass/Epoxy 600 g/m<sup>2</sup> and type E-glass/Epoxy 800 g/m<sup>2</sup>.

	10L B2-C600	12L B1-C600	14L B1-C600
Specimens			
Damaged Area, (m <sup>2</sup> )	0.000788	0.00054	0.000428
	10L B2-E800	12L B3-E800	14L B3-E800
Specimens			
Damaged Area, (m <sup>2</sup> )	0.00024	0.000212	0.000068



**Table-4.** Damage area at impact energy 48 J for type C-glass/Epoxy 600 g/m<sup>2</sup> and type E-glass/Epoxy 800 g/m<sup>2</sup>.



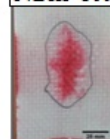


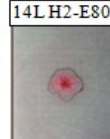
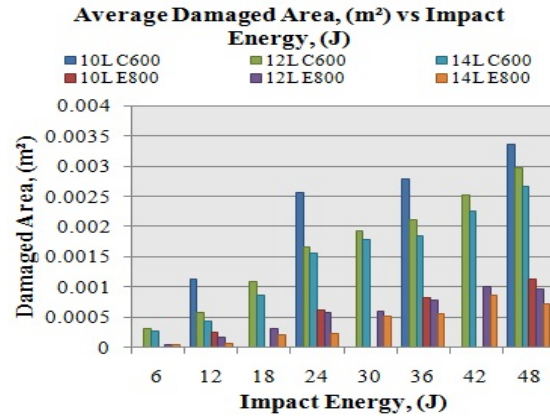
Specimens	<div>10L H2-C600</div> 	<div>12L H2-C600</div> 	<div>14L H3-C600</div> 
Damaged Area, (m <sup>2</sup> )	0.003764	0.003376	0.002688
Specimens	<div>10L H3-E800</div> 	<div>12L H2-E800</div> 	<div>14L H2-E800</div> 
Damaged Area, (m <sup>2</sup> )	0.000988	0.000992	0.000668

Table-3 and Table-4 show the damage area for both types of GFRP at two different impact energy levels. The damaged area shown are on the impacted surface of the specimen. Both tables show that as the number of plies increases, the damage areas decreases. Both tables also show that as the impact energy increases, the specimen damage area increases. Sutherland et al [37] have shown that there are generally three main 'regimes' of impact behaviour: un-delaminated, delaminated, and fibre damage. There are many different damage modes, such as matrix cracking, matrix degradation, permanent indentation, internal delamination, partial surface micro-buckling, delamination of the upper 'front-face' laminate, front-face fibre damage, fibre damage on the lower 'back-face', and perforation. A circular, internal delamination occurs for specimens impacted at 12 J for 14-ply E-glass/Epoxy 800 g/m<sup>2</sup>. A small permanent indentation occurs under the impactor. As the impact energy increases, the internal and front-face delamination areas increase, while the permanent indentation becomes more severe. Both tables show that GFRP laminate type E-glass/Epoxy 800 g/m<sup>2</sup> has experienced a smaller damaged area, compared to GFRP type C-glass/Epoxy 600 g/m<sup>2</sup>. This indicates that GFRP type E-glass/Epoxy 800 g/m<sup>2</sup> is higher in strength compared to GFRP type C-glass/Epoxy 600 g/m<sup>2</sup>.

Figure-11 shows the average damaged area for GFRP type C-glass/Epoxy 600 g/m<sup>2</sup> and type E-glass/Epoxy 800 g/m<sup>2</sup>. As the impact energy increases, the damage area also increases for all tested specimens. However, as the specimen thickness increases, the specimen damage area decreases due to the ability to absorb the impact energy [25]. According to Sevkati et al. [38], when the energy absorbed by the composite is small, the impactor bounced back and the damage area is also small. GFRP type E-glass/Epoxy 800 g/m<sup>2</sup> experienced less damaged area for all thicknesses compared to GFRP type C-glass/Epoxy 600 g/m<sup>2</sup>. This is because, GFRP type

E-glass/Epoxy 800 g/m<sup>2</sup> is higher in strength compared to GFRP type C-glass/Epoxy 800 g/m<sup>2</sup>.










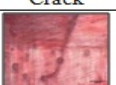

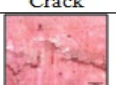


**Figure-11.** Damaged area-impact energy for type C-glass/Epoxy 600 g/m<sup>2</sup> and type E-glass/Epoxy 800 g/m<sup>2</sup>.

#### Microscopic inspection

Optical microscopy was used to investigate the impact damage of the laminates. Delamination, matrix cracking, matrix breakage, fibre cracking, and fibre breakage were observed from the microstructure of the damaged specimens.

**Table-5.** Microscopic images for type C-glass/Epoxy 600 g/m<sup>2</sup> and type E-glass/Epoxy 800 g/m<sup>2</sup>.

		Impact Energy, 12J	Impact Energy, 24J
10-ply Type C-glass/Epoxy 600 g/m <sup>2</sup>	Specimen		
	Failure Mode	Matrix Crack	Matrix Break
10-ply Type E-glass/Epoxy 800 g/m <sup>2</sup>	Specimen		
	Failure Mode	Matrix Crack	Matrix Break
12-ply Type C-glass/Epoxy 600 g/m <sup>2</sup>	Specimen		
	Failure Mode	Matrix Crack	Matrix Break
12-ply Type E-glass/Epoxy 800 g/m <sup>2</sup>	Specimen		
	Failure Mode	Delamination	Matrix Crack
14-ply Type C-glass/Epoxy 600 g/m <sup>2</sup>	Specimen		
	Failure Mode	Matrix Crack	Matrix Crack
14-ply Type E-glass/Epoxy 800 g/m <sup>2</sup>	Specimen		
	Failure Mode	Delamination	Matrix Crack





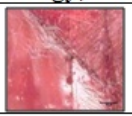
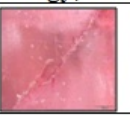
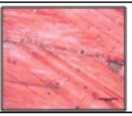
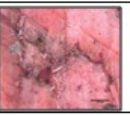
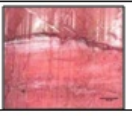

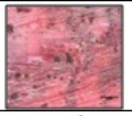
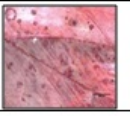
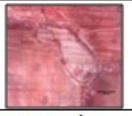
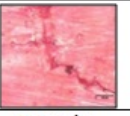

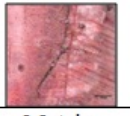
		Impact Energy, 36J	Impact Energy, 48J
10-ply Type C- glass/ Epoxy 600 g/m <sup>2</sup>	Specimen		
	Failure Mode	Fibre Crack	Fibre Break
10-ply Type E- glass/ Epoxy 800 g/m <sup>2</sup>	Specimen		
	Failure Mode	Fibre Crack	Fibre Crack
12-ply Type C- glass/ Epoxy 600 g/m <sup>2</sup>	Specimen		
	Failure Mode	Fibre Crack	Fibre Crack
12-ply Type E- glass/ Epoxy 800 g/m <sup>2</sup>	Specimen		
	Failure Mode	Matrix Crack	Fibre Crack
14-ply Type C- glass/ Epoxy 600 g/m <sup>2</sup>	Specimen		
	Failure Mode	Matrix Crack	Matrix Crack
14-ply Type E- glass/ Epoxy 800 g/m <sup>2</sup>	Specimen		
	Failure Mode	Matrix Crack	Matrix Crack

Table-5 shows the failure mode at the impacted surface area for 10-ply, 12-ply and 14-ply GFRP Type C-glass/Epoxy 600 g/m<sup>2</sup> and Type E-glass/Epoxy 800 g/m<sup>2</sup>. The 10-ply type C-glass/Epoxy 600 g/m<sup>2</sup> specimens exhibited more severe matrix damage than the other tested specimens. 14-ply Type E-glass/Epoxy 800 g/m<sup>2</sup> experienced less impact damage since it is thicker than the other tested specimens. At the energy level of 12 J, for 14-ply Type E-glass/Epoxy 800 g/m<sup>2</sup>, delamination occurs. However, for 14-ply Type C-glass/Epoxy 600 g/m<sup>2</sup>, the failure mode is matrix crack. Type C-glass/Epoxy 600 g/m<sup>2</sup> specimens exhibited more severe matrix damage than the Type E-glass/Epoxy 800 g/m<sup>2</sup> at the same impact energy level. This shows that GFRP Type E-glass/Epoxy 800 g/m<sup>2</sup> is stronger than GFRP Type C-glass/Epoxy 600 g/m<sup>2</sup>.

At impact energy 48 J, for 10-ply Type E-glass/Epoxy 800 g/m<sup>2</sup>, the failure mode is only fibre crack. However, for 10-ply Type C-glass/Epoxy 600 g/m<sup>2</sup>, the failure mode is fibre break. 14-ply Type E-glass/Epoxy 800 g/m<sup>2</sup> only experienced matrix crack and 14-ply Type

C-glass/Epoxy 600 g/m<sup>2</sup> also exhibited matrix crack when impacted at the highest impact energy, 48 J. This shows that as the number of plies increases, the failure becomes more lenient.

The damages incurred by the specimens under a 48 J impact load were more severe compared to the damages under 12 J impact loads. Several damage modes have been observed in this experiment, under a 12 J impact load, the main damage modes were delamination and matrix crack rather than fibre crack or fibre break. The damage modes of other specimens in this energy category were fibre breakage accompanied by matrix cracks, delaminations, penetrations and perforations. For higher impact energies of 48 J, fibre crack and fibre break were noticed around the site of impact. These fragmentation results were expected; the damage areas increased as the impact energy increased. For both types of GFRP, for specimens that are damaged by 12 J to 48 J impact energy, matrix cracks were observed on the damaged surface, and delaminations in the cross-section and on the inner surface of the specimens, except for 14-ply type E-glass/Epoxy 800 g/m<sup>2</sup> and 12-ply type E-glass/Epoxy 800 g/m<sup>2</sup> at impact energy 12 J.

## CONCLUSIONS

In this study, low-velocity impact tests were performed on GFRP type E-glass/Epoxy 800 g/m<sup>2</sup> and type C-glass/Epoxy 600 g/m<sup>2</sup> specimens with various thicknesses, according to the number of plies fabricated, and by varying the impact energy. From the results obtained, the peak impact force, the peak energy, the energy absorbed, the damage area, and the peak displacement increase with an increase in the impact energy for both types of GFRP. Comparing both types of GFRP at the same impact energy, type C-glass/Epoxy 600 g/m<sup>2</sup> has a lower peak force compared to type E-glass/Epoxy 800 g/m<sup>2</sup>. Therefore, GFRP type E-glass/Epoxy 800 g/m<sup>2</sup> is more impact resistant.

GFRP type E-glass/Epoxy 800 g/m<sup>2</sup> had a smaller damage area compared to type C-glass/Epoxy 600 g/m<sup>2</sup> at all impact energies tested. At the impact of 12J, 14-ply Type E-glass/Epoxy 800 g/m<sup>2</sup> only experienced delamination. Therefore, 14-ply Type E-glass/Epoxy 800 g/m<sup>2</sup> is more impact resistant. The failure mode is from delamination due to fibre cracking. The Type C-glass/Epoxy 600 g/m<sup>2</sup> specimens exhibited more severe matrix damage than the Type E-glass/Epoxy 800 g/m<sup>2</sup> at the same impact energy level. The difference in thickness and the mechanical properties for both types of GFRP do affect the impact character is action and the damaged area of the specimens tested. It can be concluded that GFRP type E-glass/Epoxy 800 g/m<sup>2</sup> is higher in strength compared to GFRP type C-glass/Epoxy 600 g/m<sup>2</sup>.

## ACKNOWLEDGEMENTS

This work is supported by UPM under GP-IPM grant, 9415402.





## REFERENCES

- [1] Vlot A. 1993. Impact properties of fiber-metal laminates. *Composite Engineering*. Vol. 3, pp. 911–927.
- [2] Vlot A. 1993. Low velocity impact loading on fiber reinforced aluminum laminates (arall and glare) and other aircraft sheet materials. Report LR-718. Delft University of Technology, pp. 36 – 38.
- [3] Belingardi G. and Vadori R. 2002. Low velocity impact tests of laminate glass-fibre-epoxy matrix composite material plates. *International Journal Impact Engineering*. Vol. 27, pp. 213–229.
- [4] Davies G. A. 1996. Impact damage and residual woven fabric glass/polyester strengths of laminates. *Composite A: Applied Science Manufacturing*. Vol. 27, pp. 1147–1156.
- [5] Zhou G. 1995. Prediction of impact damage thresholds of glass fibre reinforced laminates. *Composite Structure*. Vol. 31, pp. 185–193.
- [6] Thanomsilp C. and Hogg P. 2003. Penetration impact resistance of hybrid composites based on commingled yarn fabrics. *Composite Science Technology*. Vol. 63, pp. 467–482.
- [7] Bibo G. A. and Hogg P. J. 1998. Influence of reinforcement architecture on glass-fibre/epoxy composite systems. *Composite Science Technology*. Vol. 58, pp. 803–813.
- [8] Hausrath R. L. and Longobardo A.V. 2010. High-strength glass fibers and markets, in: Wallenberger, F. T., Bingham, P. A. (Eds.), *Fiberglass and Glass Technology: Energy-Friendly Compositions and Applications*, Springer, New York. pp. 197-225.
- [9] Vaidya U. 2011. Impact response of laminated and sandwich composites. *Impact Engineering of Composite Structures*. Vol. 526, pp. 97–191.
- [10] Sjoblom P. O., Hartness J. T. and Cordell T. M. 1988. On low velocity impact testing of composite materials. *Composite Material*. Vol. 22, pp. 30–52.
- [11] Shivakumar K.N., Elber W. and Illg W. 1985. Prediction of low velocity impact damage in thin circular laminates. *American Institute of Aeronautics and Astronautics Journal*. Vol. 23, pp. 442–449.
- [12] Mathivanan N. R. and Jerald J. 2010. Experimental Investigation of Low-velocity Impact Characteristics of Woven Glass Fiber Epoxy Matrix Composite Laminates of EP3 Grade. *Materials and Design*. Vol. 31, pp. 4553 – 4560.
- [13] Cantwell W. J. and Morton J. 1991. The Impact Resistance of Composite Materials – A review. *Composites*. Vol. 22, pp. 347 – 362.
- [14] 2002. Polymer matrix composites materials usage, design, and analysis (MIL-HDBK-17-3F). *Composite Materials Handbook*. Vol. 3, pp. 403–404.
- [15] Sultan M. T. H., Worden K., Pierce S. G., Hickey D., Staszewski W. J., Dulieu-Barton J. M. and Hodzic A. 2011. On impact damage detection and quantification for CFRP laminates using structural response data only. *Mechanical Systems and Signal Processing*. Vol. 25, pp. 3135–3152.
- [16] Nayfeh A. 1995. Wave propagation in layered anisotropic media with applications to composites. Elsevier. New York.
- [17] Cromer K., Gillespie J. W. and Keefe M. 2012. Effect of non-coincident impacts on residual properties of glass/epoxy laminates. *Journal of Reinforced Plastics and Composites*. Vol. 31, pp. 815–827.
- [18] Manikandan V., Jappes J. T. W., Kumar S. M. S. and Amuthakkannan P. 2012. Investigation of the Effect of Surface Modifications on the Mechanical Properties of Basalt Fibre Reinforced Polymer Composites. *Composites: Part B*. Vol. 43, pp. 812 – 818.
- [19] Nasirzadeh R. and Sabet A. R. 2014. Study of Foam Density Variations in Composite Sandwich Panels under High Velocity Impact Loading. *International Journal of Impact Engineering*. Vol. 63, pp. 129 – 139.
- [20] Uyaner M., Kara M. and Sahin A. 2014. Fatigue behavior of filament wound E-glass/epoxy composite tubes damaged by low velocity impact. *Composites: Part B*. Vol. 61, pp. 358–364.
- [21] Grady D. E. and Winfree N. A. 2001. Impact fragmentation of high-velocity compact projectiles on thin plates: a physical and statistical characterization of fragment debris. *International Journal Impact Engineering*. Vol. 26, pp. 249–62.
- [22] Hibbler R. C. 1989. *Engineering mechanics: statistics*. 5<sup>th</sup> ed. New York: Macmillan.
- [23] 2012. Penetrant Testing. *Applied Welding Engineering: Processes, Codes and Standards*. Elsevier, pp. 283-290.
- [24] Amaro A. M., Reis P. N. B., De Moura M. F. S. F. and Neto M. A. 2013. Influence of multi-impacts on GFRP composites laminates. *Composites: Part B*. Vol. 52, pp. 93–99.



- [25] Sultan M. T. H., Worden K., Staszewski W. J. and Hodzic A. 2012. Impact Damage Characterization of Composite Laminates Using A Statistical Approach. *Composites Science and Technology*. Vol. 72, pp. 1108 – 1120.
- [26] Davies G. A. O., Hitchings D. and Ankersen J. 2006. Predicting delamination and debonding in modern aerospace composite structures. *Composite Science Technology*, Vol. 66, pp. 846–54.
- [27] Hosur M., Chowdhury F. and Jeelani S. 2007. Low Velocity Impact Response and Ultrasonic NDE of Woven Carbon/Epoxy - Nanoclay Nanocomposites. *Journal of Composite Materials*, pp. 2195-2212.
- [28] Atas C. and Liu D. 2008. Impact response of woven composites with small weaving angles. *International Journal Impact Engineering*, Vol. 35, pp. 80–97.
- [29] Atas C., Icten B. M. and Küçük M. 2013. Thickness effect on repeated impact response of woven fabric composite plates. *Composites: Part B*. Vol. 49, pp. 80–85.
- [30] Tita V., De Carvalho J. and Vandepitte D. 2008. Failure analysis of low velocity impact on thin composite laminates: Experimental and numerical approaches. *Composite Structures*. Vol. 83, pp. 413–428.
- [31] Ghelli D. and Minak G. 2011. Low velocity impact and compression after impact tests on thin carbon/epoxy laminates. *Composites: Part B*. Vol. 42, pp. 2067–2079.
- [32] Zhang Z. Y. and Richardson M. O. W. 2007. Low velocity impact induced damage evaluation and its effect on the residual flexural properties of pultruded GRP composites. *Composite Structures*, Vol. 81, pp. 195–201.
- [33] Ude A. U., Ariffin A. K. and Azhari C. H. 2013. Impact damage characteristics in reinforced woven natural silk/epoxy composite face-sheet and sandwich foam, coremat and honeycomb materials. *International Journal of Impact Engineering*, Vol. 58, pp. 31-38.
- [34] Sutherland L. S. and Soares C. G. 2005. Impact of low fibre-volume, glass/polyester rectangular plates. *Composite Structure*, Vol. 68, pp. 13-22.
- [35] Sikarwar R. S., Velmurugan R. and Gupta N. K. 2014. Influence of fiber orientation and thickness on the response of glass/epoxy composites subjected to impact loading. *Composites: Part B*. Vol. 60, pp. 627-636.
- [36] Agrawal S., Singh K. K. and Sarkar P. K. 2014. Impact damage on fibre-reinforced polymer matrix composite - A review. *Journal of Composite Materials*. Vol. 48, p. 317.
- [37] Sutherland L. S. and Soares C. G. 2005. Impact characterization of low fibre-volume glass reinforced polyester circular laminated plates. *International Journal of Impact Engineering*. Vol. 31, pp. 1–23.
- [38] Sevkatt E., Liaw B., Delale F. and Raju B. 2010. Effect of repeated impacts on the response of plain-woven hybrid composites. *Composite: Part B*. Vol. 41, pp. 403–413.